AlN/AlGaInN superlattice light-emitting diodes at 280 nm

G. Kipshidze, V. Kuryatkov, K. Zhu, and B. Borisov
Department of Electrical and Computer Engineering, Texas Tech University, Lubbock, Texas 79409

M. Holtz
Department of Physics and NanoTech Center, Texas Tech University, Lubbock, Texas 79409

S. Nikishin[a] and H. Temkin
Department of Electrical and Computer Engineering and NanoTech Center, Texas Tech University, Lubbock, Texas 79409

(Received 5 February 2002; accepted 13 November 2002)

Ultraviolet light-emitting diodes operating at 280 nm, grown by gas source molecular-beam epitaxy with ammonia, are described. The device is composed of *n*- and *p*-type superlattices of AlN(1.2 nm thick)/AlGaInN(0.5 nm thick) doped with Si and Mg, respectively. With these superlattices, and despite the high average Al content, we obtain hole concentrations of $(0.7-1.1)\times 10^{18}\,\mathrm{cm}^{-3}$, with the mobility of 3–4 $\mathrm{cm}^2/\mathrm{V\,s}$ and electron concentrations of $3\times 10^{19}\,\mathrm{cm}^{-3}$, with the mobility of 10–20 $\mathrm{cm}^2/\mathrm{V\,s}$, at room temperature. These carrier concentrations are sufficient to form effective $p-n$ junctions needed in UV light sources. © *2003 American Institute of Physics.*
[DOI: 10.1063/1.1535255]

There has been considerable recent interest in the preparation of ultraviolet light-emitting diodes (LEDs) based on alloys of AlGaInN.[1–9] Devices with emission wavelength between 340 and 280 nm would be of interest in many applications, ranging from fluorescence excitation to data storage. However, despite recent progress, preparation of light sources operating below 300 nm is still very difficult. Limits on *p*-type doping of AlGaN with high Al concentration have been overcome to some extent by the use of AlGaN/GaN[10–12] and AlGaInN/AlGaInN[7,8] superlattices (SL), allowing for the preparation of LEDs with emission wavelength close to 300 nm. Recently, we have shown that SLs based on AlN/AlGaInN, doped with Mg, can be used to increase the effective band gap of the *p*-type cladding layer, demonstrating a 290-nm device.[9]

This work describes LEDs operating at 280 nm. These devices are based on similar *n*-type and *p*-type AlN/AlGaInN SLs. We discuss electrical and optical properties of these SLs separately and point out the importance of active structure design and careful post-growth device fabrication.

LEDs described in this work, and illustrated schematically in Fig. 1, are grown by gas source molecular-beam epitaxy with ammonia[13] on sapphire substrates. Epitaxial growth starts with the nitridation of the substrate, at 900 °C. A 40-nm-thick layer of AlN is grown first to produce a two-dimensional (2D) Al polar surface.[14] A buffer layer of AlGaN, with Al content of 0.1, is grown next. This layer, with a thickness of $\sim$1.0 μm, is grown under 2D conditions. During its growth, we calibrate growth rates using *in situ* spectroscopic pyrometry.[15] The entire device structure consists of barriers of AlN and wells of AlGaInN. The barriers are 1.2-nm thick and the wells are 0.5-nm thick, as calculated from growth rates. The Al content in the well is 0.1. The level of In incorporation, 0.05%, is estimated from the redshift of cathodoluminescence (CL) spectra of AlGaInN compared to a reference of AlGaN. The lower SL structure is doped with Si derived from silane. This *n*-type doping process is very effective and the dopant is introduced intermittently, during the growth of AlGaInN wells only. The *n*-type structure contains 150 barrier/well pairs for a total thickness of less than 300 nm. The *p*-type SL is intended to be structurally identical to the *n*-type structure. It is uniformly doped with Mg evaporated from an effusion cell. The growth is terminated with a 5-nm-thick quaternary *p*-type contact layer. The barrier and well dimensions are below their critical thickness and no additional dislocations appear to be generated in the SL itself. The crystal perfection of the SL depends strongly on the quality of the buffer layer and a more detailed study will be reported elsewhere.[16]

We have grown devices structures with two different transition regions from *n*- to *p*-type SLs, referred to in Fig. 1 as the active region. The first is an abrupt transition in which a Si-doped well is grown adjacent to a Mg-doped barrier. We refer to this type of a device as homojunction. The second design incorporates five undoped well/barrier pairs, with one monolayer wider wells, between *n*- and *p*-type SLs. This heterostructure design improves carrier confinement, and it appears to provide a region of higher radiative recombination, as discussed subsequently.

Ultraviolet CL spectra of *n*- and *p*-type SLs, grown as separate samples, as well as spectra obtained on the entire device structure, are shown in Fig. 2. Individual SL samples were grown without the AlGaN buffer layer, since these structures were also used for electrical measurements. The total thickness of each SL was increased to 0.7 μm in order to minimize the effect of surface depletion. CL measurements were carried out at an emission current of 0.1 mA, with the beam diameter of 7 mm. The electron beam voltage

[a]Author to whom correspondence should be addressed; electronic mail: Sergey.Nikishin@coe.ttu.edu

 © 2003 American Institute of Physics

Downloaded 06 Jan 2004 to 129.118.86.46. Redistribution subject to AIP license or copyright, see http://ojps.aip.org/japo/japcr.jsp

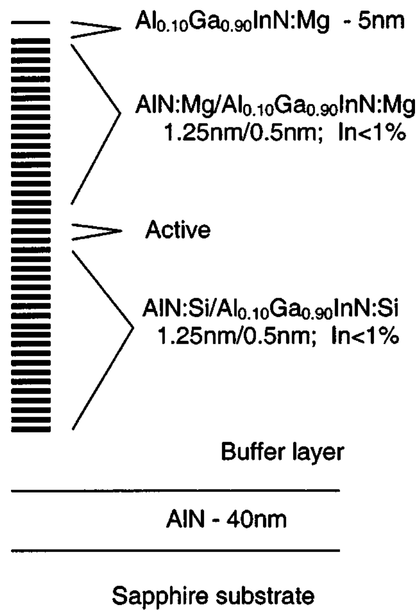

FIG. 1. Schematic cross section of the LED operating at 280 nm and based on SLs of AlN/AlGaInN.

was varied from 3 to 9 kV, resulting in the penetration depth changing from ~0.1 to ~0.7 μm. The *n*- and *p*-type SLs show ultraviolet emission at 278 nm (4.46 eV) and 282 nm (4.40 eV), respectively. The estimated effective band gap of these structures, based on the average Al content of 0.63–0.65, is close to 4.8 eV.[17] Reflectivity spectra obtained on different SLs, not shown here, indicate optical band gaps ranging from 4.6 to 5.0 eV, consistent with these estimates. The ultraviolet CL emission is thus related to the band edge. However, our estimate does not include effects of quantum confinement or mini-band formation, or band distortion (redshift) due to high interfacial electric fields. While exact identification of these features cannot be made, we interpret the CL data as the measurement of the electron–hole recombination energy expected in an LED.

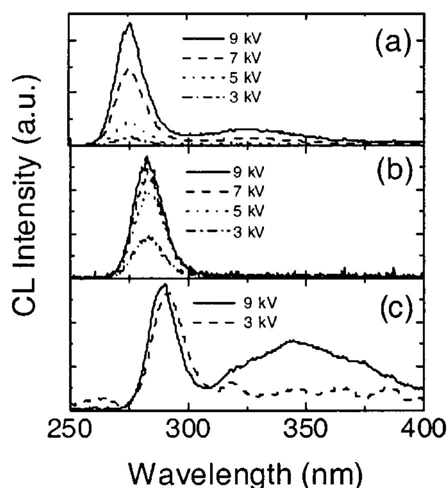

FIG. 2. Room-temperature CL spectra of (a) *n*-type, Si-doped SL as a function of the excitation voltage, (b) *p*-type, Mg-doped SL, also shown as a function of the excitation voltage, and of (c) homojunction diode structure at 3 kV, exciting mostly the top *p*-type SL, and at 9 kV, which also excites the *n*-type SL.

The difference of 60 meV observed between *n*- and *p*-type SLs is attributed to different growth rate calibrations and to the carrier concentration difference, as discussed subsequently. The CL spectrum of Fig. 2(c) is obtained on a homojunction structure. At low excitation voltage of 3 kV, most of the signal originates in the *p*-type SL. At higher voltage of 9 kV, the signal originates from both SLs. The edge-related emission in this sample is visible at ~290 nm, and the spectra at two excitation voltages, arising from two different SLs, are shifted by ~30 meV. This result does not change when different areas of the wafer are probed, indicating a high degree of sample uniformity. In addition, CL spectra obtained at 9 kV show a broad peak, redshifted by ~670 meV, similar to that observed in the Si-doped SLs of Fig. 2(a). The substructure of this peak is not resolved at room temperature. Introduction of an undoped barrier/well region does not change the CL spectra of LED structures but, as shown later, has a large effect on electroluminescence.

Hall measurements on the SLs of Figs. 2(a) and 2(b) were carried out in the temperature range of 77 to 300 K. These samples were not annealed after the growth. The room-temperature electron concentration in the *n*-type SL reaches $3\times10^{19}\,\mathrm{cm}^{-3}$ with the mobility of 10–20 $\mathrm{cm^2/V\,s}$ and the resistivity of $0.015\pm0.005\ \Omega\,\mathrm{cm}$. The room-temperature hole concentration in the *p*-type SL reaches $(0.7-1.1)\times10^{18}\,\mathrm{cm}^{-3}$ with the mobility of 3–4 $\mathrm{cm^2/V\,s}$ and resistivity of ~2 $\Omega\,\mathrm{cm}$. Hall resistivities are very weakly temperature dependent. However, in contrast to in-plane 2D gas structures[12] the carrier transport in our SLs occurs in thin wells and impurity scattering cannot be completely removed. In addition, Hall measurement determines the in-plane mobility and resistivity, while in LED it is the mobility in the direction perpendicular to the SL plane that is important. These results demonstrate the value of using AlN/AlGaInN SLs as highly doped cladding layers in light-emitting devices.

The relative blueshift of the *n*-type SL visible in the CL spectrum of the diode structure shown in Fig. 2(c) appears to be due to high carrier concentration. This results in screening of the interfacial electric field distorting the SL, the quantum confined Stark effect. Given the well thickness of 0.5 nm, the average carrier concentration of $3\times10^{19}\,\mathrm{cm}^{-3}$, and using the dielectric constant of GaN of 8.9,[18] a screening field of 6×10^{5} V/cm is estimated. This results in a blueshift, a product of the field and the well thickness, of ~30 meV, in good agreement with the data of Fig. 2(c). Thus, at least a part of the blueshift between *n*- and *p*-type SLs seen in the CL data of Figs. 2(a) and 2(b) can be attributed to this effect.

Electroluminescence (EL) results obtained on our LEDs exhibit complex behavior, strongly influenced by the design of the active region and the device fabrication procedure, as shown in Fig. 3. Preliminary measurements were carried out on devices prepared simply by depositing Ni contact dots with two different diameters, 70 and 500 μm, on the *p*-type surface. The large diameter contact serves as a cathode. Light is collected with a UV-transparent fiber from the edge of the small dot, the *p*-type contact, and analyzed with a spectrom-

Downloaded 06 Jan 2004 to 129.118.86.46. Redistribution subject to AIP license or copyright, see http://ojps.aip.org/japo/japcr.jsp

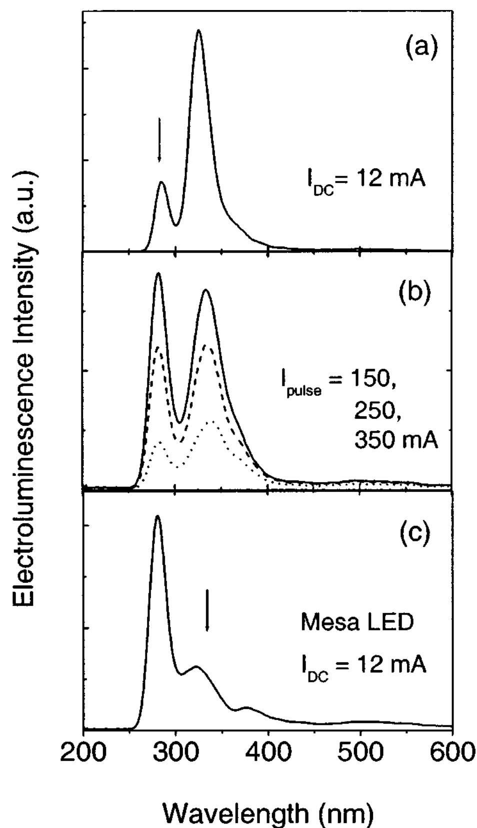

FIG. 3. Room-temperature EL spectra of (a) LED test structure with *n*-type SL grown without Si doping, (b) LED structure with an active region formed by five undoped well/barrier pairs, under pulsed excitation ($\tau_{pulse} = 50\ \mu s$ and the duty factor of 0.005), and (c) mesa structure LED with the active region structure same as that of (b).

eter. No light is observable around the large contact dot. EL spectra of homojunction-type diodes, grown with an abrupt *n*- to *p*-type transition, obtained with this arrangement, exhibit only the 320–350 nm emission (not shown in Fig. 3). This peak appears to correlate with that seen in CL measurements of Si-doped SLs, shown in Figs. 2(a) and 2(c). Figure 3(a) shows the EL spectrum obtained on a control structure, grown without Si doping. The dominant emission still occurs at ~330 nm but a second peak, at 280 nm, is also present. Light emission is visible at forward dc currents as low as 2 mA (at $V_f \sim 10$ V) and the 280-nm peak increases rapidly with forward current. However, the forward dc current is limited to ~30 mA, and pulsed current to ~80 mA, by high series resistance of this structure. Figure 3(b) shows the EL spectra of a structure that incorporates five undoped well/barrier pairs between SLs doped with Si and Mg. This structure also shows two peaks, at 280 and 330 nm. When driven with pulsed current, up to 350 mA, the intensity of the 280 nm begins to dominate. The spectrum of Fig. 3(c) was obtained on the same structure, with five undoped barrier/well pairs, after 0.5–0.6-μm-deep mesas were etched around contact dots, through the $p-n$ junction that is estimated to be ~0.3-μm deep. The mesas were plasma etched with Cl-chemistry using Ni contacts as masks. Electrical probes were again placed on adjacent large and small Ni dots. EL spectra of the etched structure show predominant emission at 280 nm, with the 330-nm line reduced to a shoulder, at all currents. Mesa-etching of Si-doped homojunction structures does not change their emission spectra.

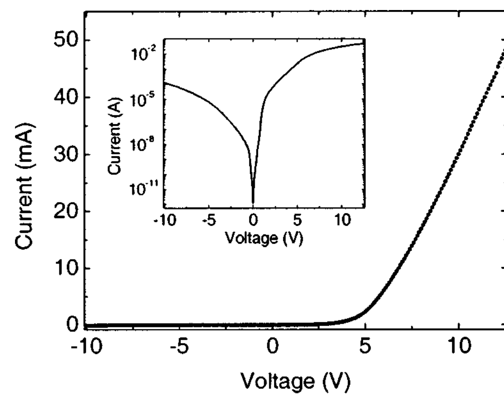

FIG. 4. Room-temperature $I-V$ characteristics of a mesa-defined LED. Inset shows $I-V$ plotted on a logarithmic scale in order to demonstrate low leakage at zero bias.

Two conclusions can be drawn from the EL data of Fig. 3. A simple configuration of metal dots on the *p*-type surface leads to large leakage current through the entire device. This is not surprising given the nature of SL structures that provide high in-plane conductance. The relative intensity of the 330-nm peak correlates with leakage current as well as the presence of Si at the junction. The presence of Si results in emission deeper than that expected on the basis of the Si donor level energy extrapolated from GaN.[18,19] Once the Si is pushed back, by incorporation of undoped active region, the competing near band-edge emission at 280 nm takes over. In such a test structure the mesa etching is effective in eliminating lateral conduction. In the vertical conduction, two effects need to be considered. The junction is of the $p-n^+$ type and that implies recombination at the *p*-side. On the other hand, diffusion length of minority electrons in the *p*-type material might be smaller than that of minority holes. This is the case in GaN.[20,21] The presence of a Si-related peak in EL spectra suggest that a similar situation might arise in AlN/AlGaInN SLs. Formation of an active region with better carrier confinement is needed in order to answer these questions. Such an active region can be formed, without affecting the emission wavelength, by increasing the effective band gap of the *n*- and *p*-type SLs or by the introduction of thicker AlN barriers around the undoped recombination region.

Electrical measurements were carried out on mesa-defined diodes with a well defined out-of-plane conduction path. The mesas, 110 μm in diameter, were plasma etched with Cl_2.[22] High *p*- and *n*-type concentrations in as-grown layers make it possible to prepare Ni/Au and Ti/Al/Ti/Au ohmic contacts without high-temperature activation anneals. The $I-V$ characteristics representative of our SL diodes are plotted in Fig. 4. The device turns on at ~5.6 V, consistent with the active layer band gap of ~4.8 eV, with a series resistance of ~ 130 Ω. This includes contact resistance to the SL, which has not been optimized yet. It is also possible that the resistivity for vertical current transport is higher than that inferred from in-plane Hall measurement. Light emission was observed at a bias greater that 6.5 V. The inset of Fig. 4

Downloaded 06 Jan 2004 to 129.118.86.46. Redistribution subject to AIP license or copyright, see http://ojps.aip.org/japo/japcr.jsp

shows the $I-V$ on a logarithmic scale. Very low dark leakage current, 2–3 pA, was measured near zero bias, indicative of high-quality junction and low etch-induced damage on the mesa sidewalls. The reverse leakage current remained below 200 μA up to a bias of -10 V.

In summary, we describe 280-nm LEDs based on *n*- and *p*-type superlattices of AlN/AlGaInN. The use of AlN-based superlattices doped with Si and Mg results in high carrier concentrations needed to prepare effective $p-n$ junction in wide band-gap nitrides.

ACKNOWLEDGMENTS

This work is supported by DARPA (under a contract monitored by Dr. J. Carrano), SBCCOM, NSF (Grant No. ECS-0070240), CRDF (Grant No. RE1-2217), NATO Science for Peace Program (Grant No. SfP-974505), and the J. F Maddox Foundation. We thank Riber Inc. for an extended cold lip Al effusion cell used for epitaxy in this work. We also thank Dr. A. S. Zubrilov for productive discussions.

[1] K. Tadamoto, H. Okagawa, Y. Ohuchi, T. Tsunekawa, Y. Imada, M. Kato, and T. Taguchi, Jpn. J. Appl. Phys. **40**, L583 (2001).
[2] T. Nishida, H. Saito, and N. Kobayashi, Appl. Phys. Lett. **78**, 3927 (2001).
[3] T. Nishida, H. Saito, and N. Kobayashi, Appl. Phys. Lett. **79**, 711 (2001).
[4] A. Kinoshita, H. Hirayama, M. Ainoya, Y. Aoyagi, and A. Hirata, Appl. Phys. Lett. **77**, 175 (2000).
[5] H. Hirayama, A. Kinoshita, and Y. Ayoagi, RIKEN Rev. **33**, 28 (2001).
[6] H. Hirayama, A. Kinoshita, A. Hirata, and Y. Ayoagi, Phys. Status Solidi A **188**, 83 (2001).
[7] M. A. Khan, V. Adivarahan, J. P. Zhang, C. Chen, E. Kuokstis, A. Chitnis, M. Shatalov, J. Wei, and G. Simin, Jpn. J. Appl. Phys. **40**, L1308 (2001).
[8] V. Adivarahan, A. Chitnis, J. P. Zhang, M. Shatalov, J. W. Yang, G. Simin, and M. A. Khan, Appl. Phys. Lett. **79**, 4240 (2001).
[9] G. Kipshidze, V. Kuryatkov, B. Borisov, M. Holtz, S. Nikishin, and H. Temkin, Appl. Phys. Lett. **80**, 3682 (2002).
[10] P. Kozodoy, M. Hansen, S. P. DenBaars, and U. K. Mishra, Appl. Phys. Lett. **74**, 3681 (1999).
[11] K. Kumakura and N. Kobayashi, Jpn. J. Appl. Phys. **38**, L1012 (1999).
[12] K. Kumakura, T. Makimoto, and N. Kobayashi, Jpn. J. Appl. Phys. **39**, 2428 (1999).
[13] N. Grandjean, B. Damilano, and J. Massies, J. Phys.: Condens. Matter **13**, 6945 (2001), and references therein.
[14] G. Kipshidze, V. Kuryatkov, K. Choi, Ìu. Gherasoiu, B. Borisov, S. Nikishin, M. Holtz, D. Tsvetkov, V. Dmitriev, and H. Temkin, Phys. Status Solidi B **188**, 881 (2001).
[15] S. A. Nikishin, S. Francoeur, and H. Temkin, Mater. Res. Soc. Symp. Proc. **639**, G.6.57.1 (2001).
[16] S. A. Nikishin (unpublished).
[17] S. A. Nikishin, N. N. Faleev, A. S. Zubrilov, V. G. Antipov, and H. Temkin, Appl. Phys. Lett. **76**, 3028 (2000).
[18] *Properties of advanced semiconductor materials: GaN, AlN, InN, SiC, SiGe*, edited by M. E. Levinstein, S. L. Rumyantsev, and M. S. Shur (Wiley, New York, 2001).
[19] T. Suski, P. Perlin, C. Skierbiszewski, P. Wisniewski, L. Dmowski, M. Leszczynski, and W. Walukiewicz, Phys. Status Solidi A **216**, 521 (1999), and references therein.
[20] L. Chernyak, A. Osinsky, H. Temkin, J. W. Yang, Q. Chen, and M. A. Khan, Appl. Phys. Lett. **69**, 2531 (1996).
[21] J. S. Speck and S. J. Rosner, Physica B **273–274**, 24 (1999).
[22] V. V. Kuryatkov, G. D. Kipshidze, S. A. Nikishin, P. W. Deelman, and H. Temkin, Phys. Status Solidi A **188**, 317 (2001).

Downloaded 06 Jan 2004 to 129.118.86.46. Redistribution subject to AIP license or copyright, see http://ojps.aip.org/japo/japcr.jsp